Fermi hypernetted-chain evaluation of a generalized momentum distribution for model nuclear matter

E. Mavrommatis and M. Petraki
Physics Department, Division of Nuclear and Particle Physics, University of Athens, Panepistimioupoli, 157 71 Athens, Greece

J. W. Clark
McDonnell Center for the Space Sciences and Department of Physics, Washington University, St. Louis, Missouri 63130
(Received 10 November 1994)

The generalized momentum distribution $n(\mathbf{p},\mathbf{Q})$, related to the half-diagonal two-body density matrix $\rho_{2h}(\mathbf{r}_1,\mathbf{r}_2,\mathbf{r}_1')$ by Fourier transformation in the variables $\mathbf{r}_1-\mathbf{r}_1'$ and $\mathbf{r}_1-\mathbf{r}_2$, plays a key role in the description of final-state interactions in the nuclear medium and other strongly interacting many-body systems. The function $n(\mathbf{p},\mathbf{Q})$ is explored for two Jastrow-correlated models of infinite nuclear matter within a Fermi hypernetted-chain procedure. Significant departures from ideal Fermi gas behavior in certain kinematic domains provide signatures of the strong short-range correlations contained in these models. However, such deviations are less prominent than in earlier calculations based on low-order cluster truncations; correspondingly, violations of the sequential relation are greatly reduced. Simple prescriptions for improved low-cluster-order approximations to $n(\mathbf{p},\mathbf{Q})$ are suggested by analysis of the results of the Fermi hypernetted-chain evaluation. These results are also used to assess the quality of Silver's approximation $n(\mathbf{p},\mathbf{Q}) \approx n(p)[S(Q)-1]$ for the generalized momentum distribution in terms of the ordinary momentum distribution $n(p)$ and the static structure function $S(Q)$, with findings that have potential implications for the interpretation of data from inclusive electron scattering by nuclei at high momentum transfers.

PACS number(s): 21.65.+f, 67.40.Db, 25.30.Fj, 24.10.Cn

I. INTRODUCTION

Substantial efforts have been directed toward both experimental determination and microscopic evaluation of the momentum distribution $n(p)$ and the associated one-body density matrix $\rho_1(\mathbf{r}_1,\mathbf{r}_1')$ of nuclear matter and finite nuclei [1–3]. As a logical next step, variational theory has been extended to permit tractable investigation of the half-diagonal two-body density matrix $\rho_{2h}(\mathbf{r}_1,\mathbf{r}_2,\mathbf{r}_1')$ of the ground states of infinite symmetrical nuclear matter and other uniform Fermi systems in strong interaction [4]. For some purposes, it is advantageous to work instead with a Fourier-space counterpart $n(\mathbf{p},\mathbf{Q})$ of ρ_{2h}. Initial calculations of the generalized momentum distribution $n(\mathbf{p},\mathbf{Q})$ have recently been performed [5] for simple models of nuclear matter defined by Jastrow-correlated wave functions, applying low-order cluster approximations within the theory of Ref. [4].

There is growing interest in $n(\mathbf{p},\mathbf{Q})$ and $\rho_{2h}(\mathbf{r}_1,\mathbf{r}_2,\mathbf{r}_1')$ as descriptors of the correlation structure of finite nuclei. This interest is stimulated by a variety of recent and projected experimental studies of inclusive quasielastic (e,e') scattering [6] and exclusive $(e,e'N)$ or $(e,e'2N)$ reactions [7,8], as well as proton scattering [9], pion absorption [10], etc. Proper interpretation of the results of these experiments and reliable extraction of useful information on momentum distributions, spectral functions, and transparency entail quantitative "post-mean-field" treatment of the propagation of ejected nucleons and their final-state interactions. Treatments of this kind include, for example, extensions of Glauber theory [11–17], and adaptation of Silver's hard-core perturbation theory to the nuclear medium [18], along with other proposed approaches [3,19]. The half-diagonal and diagonal portions of the two-body density matrix figure prominently in most of these analyses. The function $\rho_{2h}(\mathbf{r}_1,\mathbf{r}_2,\mathbf{r}_1')$, or alternatively $n(\mathbf{p},\mathbf{Q})$, is also involved in fundamental sum rules that furnish insights into the nature of the elementary excitations of quantum many-body systems [20].

We consider uniform, isospin-symmetrical, spin-saturated nuclear matter at density ρ, with corresponding Fermi wave number $k_F=(6\pi^2\rho/\nu)^{1/3}$, where $\nu=4$ is the level degeneracy of plane-wave single-particle states. For a given state vector $|\Psi\rangle$, the generalized momentum distribution $n(\mathbf{p},\mathbf{Q})$ of the system is defined by

$$n(\mathbf{p},\mathbf{Q})=\sum_{\hat{\mathbf{k}}}\langle\Psi|a^\dagger_{\hat{\mathbf{k}}+\mathbf{Q}}a^\dagger_{\hat{\mathbf{p}}-\mathbf{Q}}a_{\hat{\mathbf{p}}}a_{\hat{\mathbf{k}}}|\Psi\rangle \quad . \tag{1}$$

Here, $\hat{\mathbf{k}}$ labels the single-particle orbital with wave vector $\mathbf{k}$ and spin/isospin projections σ,τ, while $\hat{\mathbf{k}}+\mathbf{Q}=(\mathbf{k}+\mathbf{Q},\sigma,\tau)$. The function $n(\mathbf{p},\mathbf{Q})$ is connected to the half-diagonal two-body density matrix

$$\rho_{2h}(\mathbf{r}_1,\mathbf{r}_2,\mathbf{r}_1')=A(A-1)\int\Psi^*(\mathbf{r}_1,\mathbf{r}_2,\mathbf{r}_3,\ldots,\mathbf{r}_A)$$

$$\times\Psi(\mathbf{r}_1',\mathbf{r}_2,\mathbf{r}_3,\ldots,\mathbf{r}_A)d\mathbf{r}_3\ldots d\mathbf{r}_A \tag{2}$$

by the Fourier transformation

$$n(\mathbf{p},\mathbf{Q}) = \frac{1}{\nu}\frac{\rho}{A}\int \rho_{2h}(\mathbf{r}_1,\mathbf{r}_2,\mathbf{r}_1')\, e^{-i\mathbf{p}\cdot(\mathbf{r}_1-\mathbf{r}_1')}\, e^{-i\mathbf{Q}\cdot(\mathbf{r}_1-\mathbf{r}_2)} \times d\mathbf{r}_1 d\mathbf{r}_2 d\mathbf{r}_1' \quad . \tag{3}$$

[In writing (2), we suppress spin/isospin labels, as well as a sum over all spin/isospin variables.] For the noninteracting system, $n(\mathbf{p},\mathbf{Q})$ reduces to

$$n_F(\mathbf{p},\mathbf{Q}) = \delta_{Q0}(A-1)\Theta(k_F-p) - (1-\delta_{Q0}) \times \Theta(k_F-p)\Theta(k_F-|\mathbf{p}-\mathbf{Q}|) \quad . \tag{4}$$

The role played by the generalized momentum distribution in final-state interactions becomes more evident if definition (1) is recast as

$$n(\mathbf{p},\mathbf{Q}) = \langle\Psi|\rho_{\mathbf{Q}} a^\dagger_{\hat{\mathbf{p}}-\mathbf{Q}} a_{\hat{\mathbf{p}}}|\Psi\rangle - n(p) \quad , \tag{5}$$

where $\rho_{\mathbf{Q}}$ is the density fluctuation operator $\sum_{\hat{\mathbf{k}}} a^\dagger_{\hat{\mathbf{k}}+\mathbf{Q}} a_{\hat{\mathbf{k}}}$ and $n(p)$ is the single-particle momentum distribution. The first term on the right may be viewed as a transition matrix element for scattering of a particle from orbital $\hat{\mathbf{p}} = (\mathbf{p},\sigma',\tau')$ into another orbital $\hat{\mathbf{p}}-\mathbf{Q} = (\mathbf{p}-\mathbf{Q},\sigma',\tau')$, this process being induced by a density fluctuation of wave vector $\mathbf{Q}$.

Along with time-reversal invariance, the generalized momentum distribution $n(\mathbf{p},\mathbf{Q})$ has the following formal properties. The relation $\rho_{2h}(\mathbf{r}_1,\mathbf{r}_2,\mathbf{r}_1) = \rho^2 g(r_{12})$ between the half-diagonal two-body density matrix and the radial distribution function $g(r)$ leads to the so-called $\mathbf{p}$ sum rule [4,21]

$$A^{-1}\sum_{\hat{\mathbf{p}}} n(\mathbf{p},\mathbf{Q}) = A\delta_{Q0} + S(Q) - 1 \quad , \tag{6}$$

where $S(Q)$ is the static structure function. In the case of strong short-range repulsions, $n(\mathbf{p},\mathbf{Q})$ also obeys the $\mathbf{Q}$ sum rule [4,21]

$$\sum_{\mathbf{Q}} n(\mathbf{p},\mathbf{Q}) = 0 \quad . \tag{7}$$

The sequential relation

$$\int \rho_{2h}(\mathbf{r}_1,\mathbf{r}_2,\mathbf{r}_1')\, d\mathbf{r}_2 = (A-1)\rho_1(\mathbf{r}_1,\mathbf{r}_1') \tag{8}$$

between ρ_{2h} and the one-body density matrix $\rho_1(\mathbf{r}_1,\mathbf{r}_1')$ may be transformed to momentum space to yield a connection between the generalized momentum distribution and the familiar momentum distribution $n(p)$:

$$n(\mathbf{p},\mathbf{Q}=0) = (A-1)n(p) \quad . \tag{9}$$

Three simple approximations [22–24] have been proposed for estimating $n(\mathbf{p},\mathbf{Q})$. In particular, Silver's approximation [23] reads

$$n(\mathbf{p},\mathbf{Q}) \approx n(p)[S(Q)-1] \quad . \tag{10}$$

This form obeys the $\mathbf{p}$ and $\mathbf{Q}$ sum rules and meets the sequential relation, but violates time-reversal invariance.

Ristig and Clark have developed techniques for evaluating $n(\mathbf{p},\mathbf{Q})$ and $\rho_{2h}(\mathbf{r}_1,\mathbf{r}_2,\mathbf{r}_1')$ at the variational level of correlated-basis-functions (CBF) theory, for both Bose and Fermi systems [21,4]. The detailed analyses are based on trial ground-state wave functions of Jastrow or Jastrow-Slater type,

$$\Psi(1,\ldots,A) = \mathcal{N}^{-1}\prod_{i<j}^{A} f(r_{ij})\,\Phi(1,\ldots,A) \quad , \tag{11}$$

where Φ is a constant (Bose system) or a Slater determinant of plane-wave orbitals filling a Fermi sea (Fermi case), $f(r_{ij})$ is a two-body correlation function healing to unity at large separations r_{ij}, and $\mathcal{N}$ is a normalization constant. Cluster-diagrammatic decomposition was followed by graphical resummations to yield structural formulas for $\rho_{2h}(\mathbf{r}_1,\mathbf{r}_2,\mathbf{r}_1')$ and for $n(\mathbf{p},\mathbf{Q})$ (which in fact are of general validity in the Bose case, transcending the Jastrow choice of correlated ground state). In particular, the function $n(\mathbf{p},\mathbf{Q})$ is cast as a sum of terms that can be physically associated with various scattering processes in the medium. The form factors, momentum distributions, and other quantities specifying these terms can be computed either by cluster expansion to some (low) order or by Bose or Fermi hypernetted-chain (HNC) techniques [25–28]. The renormalized (Bose or Fermi) expression for $n(\mathbf{p},\mathbf{Q})$ exhibits a sum-of-products structure built up from certain irreducible-diagram sets of HNC theory.

In Ref. [5], numerical calculations of $n(\mathbf{p},\mathbf{Q})$ within this framework were begun for nuclear matter described by a Jastrow-Slater wave function. Two approximation schemes were investigated:

(i) *LO Approximation.* Evaluation to lowest (two-body) cluster order in the raw cluster expansion generated for $n(\mathbf{p},\mathbf{Q})$ directly from the definition (1) (see Fig. 2 of Ref. [5] or Fig. 4 of Ref. [4] for a diagrammatic representation of this approximation).

(ii) *LOIC1 Approximation.* Lowest-cluster-order evaluation of the form factors (and other ingredients) of the renormalized structural expression for $n(\mathbf{p},\mathbf{Q})$ appropriate to the Fermi problem [see Eq. (12) below].

The pilot studies of Ref. [5] show very substantial deviations from the baseline case (4) of the noninteracting Fermi gas. A detailed examination and comparison of individual contributions to these deviations, for models of nuclear matter with different correlation strengths, indicates that neglected cluster terms of higher order may be quite important. This conclusion is supported by the occurrence of large violations of the sequential condition (9). It therefore seems advisable to proceed to a Fermi hypernetted-chain (FHNC) treatment of $n(\mathbf{p},\mathbf{Q})$. The purpose of this paper is to carry out such an evaluation at the FHNC/0 level in which elementary or bridge diagrams are omitted. Section II recapitulates the framework of our calculation. Two simple nuclear-matter mod-

els are specified in Sec. III, and the numerical results for these models are presented and discussed in Sec. IV. Some directions for future work are identified in Sec. V.

II. FERMI HYPERNETTED-CHAIN ANALYSIS

For a Fermi system described by a Jastrow-Slater wave function, well-known techniques [28] may be used to develop a cluster expansion of the generalized momentum distribution $n(\mathbf{p},\mathbf{Q})$ in the thermodynamic limit ($A \sim \infty$, $\rho = \text{const}$). One obtains an infinite series whose addends are generally *reducible*, in that they are represented as *products* of cluster diagrams. Resummation of graphical subseries leads to a closed-form expression for $n(\mathbf{p},\mathbf{Q})$ in terms of a small number of irreducible quantities [4]. The resummation processes are most readily carried out in configuration space, taking advantage of simple asymptotic behaviors and transparent relations to the Bose problem [21]. Returning to Fourier space, the resulting structural expression is

$$\begin{aligned} n(\mathbf{p},\mathbf{Q}) = {} & (A-1)\delta_{Q0}n(p) + (1-\delta_{Q0})F_{dd}(Q)[n(p)+n(|\mathbf{p}-\mathbf{Q}|)] + (1-\delta_{Q0})F_{de}(Q)[n_{Dl}(p)+n_{Dl}(|\mathbf{p}-\mathbf{Q}|)] \\ & -n_0(1-\delta_{Q0})[\Theta(k_F-p)-F_{cc}(p)][\Theta(k_F-|\mathbf{p}-\mathbf{Q}|)-F_{cc}(|\mathbf{p}-\mathbf{Q}|)] \\ & +(1-\delta_{Q0})n^{(2)'}(\mathbf{p},\mathbf{Q}) + (1-\delta_{Q0})n^{(3)'}(\mathbf{p},\mathbf{Q}) \quad . \end{aligned} \tag{12}$$

The ingredients of this formula, namely n_0, $n(k)$, $n_{Dl}(k)$, $F_{xy}(k)$, $n^{(2)'}(\mathbf{p},\mathbf{Q})$, and $n^{(3)'}(\mathbf{p},\mathbf{Q})$, are all susceptible to calculation by Fermi hypernetted-chain (FHNC) procedures [4]. In this list, n_0 is the strength factor that occurs in the structural formula [25–27] for the ordinary momentum distribution $n(k)$ (itself a reducible quantity). The modified momentum distribution $n_{Dl}(k)$ (likewise reducible) is defined by

$$n_{Dl}(p) = \frac{1}{\nu}\int \rho_{1D}(r)l(r)\,e^{i\mathbf{p}\cdot\mathbf{r}}d\mathbf{r} \quad , \tag{13}$$

where $\rho_{1D}(r)$ is the direct-direct (dd) component of the full Fermi one-body density matrix $\rho_1(\mathbf{r}_1,\mathbf{r}_1')$. In addition, we have the "two-point" quantities $F_{xy}(k)$ (with $xy = dd$, de, or cc), which serve as form factors, and the "three-point" quantities $n^{(2)'}(\mathbf{p},\mathbf{Q})$ and $n^{(3)'}(\mathbf{p},\mathbf{Q})$. The designations "two-point" and "three-point" refer to the graphical topology of the corresponding configuration-space functions entering Fourier transformations such as

$$F_{xy}(k) = \rho\int F_{xy}(r)\,e^{i\mathbf{k}\cdot\mathbf{r}}\,d\mathbf{r} \quad . \tag{14}$$

The form factors $F_{xy}(r)$ have the composition

$$F_{xy}(r) \equiv F_{Qxy}(r) = X_{Qxy}(r) + N_{Qxy}(r) \quad , \tag{15}$$

and thus can be evaluated in terms of the nodal (N_Q) and non-nodal (X_Q) diagram sets that arise in the FHNC analysis of the one-body density matrix [26,27]. (The Q index appearing in Eq. (15) is introduced temporarily to make the necessary connection with Ristig's notation [27]; it should not be confused with the momentum variable Q.) The three-point quantity $n^{(2)'}(\mathbf{p},\mathbf{Q})$ is given by a three-dimensional integral over a sum of products of two-point functions,

$$n^{(2)'}(\mathbf{p},\mathbf{Q}) = \frac{1}{\nu}\frac{\rho}{A}\int K(\mathbf{r}_1,\mathbf{r}_2,\mathbf{r}_1')\,e^{-i\mathbf{p}\cdot(\mathbf{r}_1-\mathbf{r}_1')}\,e^{-i\mathbf{Q}\cdot(\mathbf{r}_1-\mathbf{r}_2)}d\mathbf{r}_1 d\mathbf{r}_2 d\mathbf{r}_1' \quad , \tag{16}$$

where (with $r \equiv |\mathbf{r}_1-\mathbf{r}_2|$ and $r' \equiv |\mathbf{r}_1'-\mathbf{r}_2|$)

$$\begin{aligned} K(\mathbf{r}_1,\mathbf{r}_2,\mathbf{r}_1') = {} & \rho\rho_1(\mathbf{r}_1,\mathbf{r}_1')F_{dd}(r)F_{dd}(r') + \rho\rho_{1D}(\mathbf{r}_1,\mathbf{r}_1')l(\mathbf{r}_1,\mathbf{r}_1')[F_{dd}(r)F_{de}(r')+F_{dd}(r')F_{de}(r)] \\ & -\nu\rho[\rho_{1D}(\mathbf{r}_1,\mathbf{r}_1')-\rho n_0][\nu^{-1}l(r)-F_{cc}(r)][\nu^{-1}l(r')-F_{cc}(r')] \quad . \end{aligned} \tag{17}$$

The remaining three-point quantity $n^{(3)'}(\mathbf{p},\mathbf{Q})$ is an integral over a sum of terms, each of which involves at least one irreducible three-point function [4]. At any rate, by extracting various results from FHNC analyses of the one-body density matrix and of the radial distribution function, one may assemble the corresponding FHNC result for $n(\mathbf{p},\mathbf{Q})$. The FHNC equations that must be solved are too lengthy to repeat in this presentation; the interested reader may find the detailed expressions in Refs. [4,26,27]. Here we implement FHNC theory at the level in which elementary diagrams (also called bridge diagrams) are not included (FHNC/0). The elementary contributions are generally expected to be important only at higher densities and are commonly ignored in calculations on nuclear systems [28,29]. By similar reasoning, the three-point quantity $n^{(3)'}(\mathbf{p},\mathbf{Q})$ should be small compared to the other terms in the $Q \neq 0$ portion of (12) and will be omitted in our calculations.

We pause in the development to point out that the resummed structural formula (12) gives clear expression to the physical content of the generalized momentum distribution, by collecting into separate addends the contributions from various virtual scattering processes. The first term recaptures the trivial result for dynamically

and statistically uncorrelated particles, with the important distinction that the momentum distribution function $n(p)$ of the fully correlated Fermi system is to be used. The correlations existing in the interacting fluid allow a fermion to scatter (virtually) from orbital $\hat{\mathbf{p}}$ to another orbital $\hat{\mathbf{p}} - \mathbf{Q}$, through the (virtual) creation of a momentum-conserving phonon of wave vector $\mathbf{Q}$. This process and its time-reversed counterpart are represented analytically by the second term in (12), which involves the direct form factor $F_{dd}(Q)$. The associated exchange-scattering effects are incorporated by the third term, involving instead the exchange form factor $F_{de}(Q)$. The fourth term takes account of the kinematic effect of the Pauli exclusion principle. This effect is also present in noninteracting cases [cf. Eq. (4)], but it is now corrected by the dynamical correlations in Jastrow approximation. More specifically, the circular-exchange function $F_{cc}(k)$ corrects for the population of states outside the Fermi sea by the interactions. The strong dynamical correlations are also responsible for an overall reduction of the Pauli kinematic effect via the strength factor n_0 $(0 \leq n_0 \leq 1)$, which reflects the depletion of the Fermi sea. The last two terms of (12) account for virtual processes of more complicated types.

In detail, the renormalized expression (12) assumes that the sequential relation (9) is satisfied. In terms of the ingredients of Eq. (12), this condition is equivalent to

$$2F_{dd}(0)n(p) + 2F_{de}(0)n_{Dl}(p) - n_0[\Theta(k_F - p) - F_{cc}(p)]^2 + n^{(2)'}(\mathbf{p},0) + n^{(3)'}(\mathbf{p},0) = -n(p)\,. \quad (18)$$

The FHNC/0 evaluation necessarily compromises the sequential relation (9) [and hence Eq. (18)] to some extent, due to the absence of elementary diagrams. For the same reason, it also fails to meet the $\mathbf{p}$ sum rule (6) (although the violation may be small). On the other hand, the FHNC/0 approximation does conserve time-reversal invariance and obeys the $\mathbf{Q}$ sum rule (7).

III. MODELS OF THE NUCLEAR MEDIUM

Numerical calculations of the generalized momentum distribution are carried out for two simple models of nuclear matter near its saturation density. These models provide a representative picture of the short-range repulsive correlations present in nuclear systems. However, the intermediate- and long-range correlations are at best described in an average-propagator approximation [30], which cannot adequately account for the strong state dependence of the realistic nucleon-nucleon interaction and especially the noncentral components of the force. Both models refer to the density value $\rho = 0.182$ fm^{-3}, corresponding to $k_F = 1.392$ fm^{-1}.

The "Monte Carlo" (MC) model is specified by the correlation function

$$f(r) = \exp\left[-C_1\, e^{-C_2 r}\, \frac{(1 - e^{r/C_3})}{r}\right] \qquad \text{(MC)} \quad (19)$$

with parameter values $C_1 = 1.7$ fm, $C_2 = 1.6$ fm^{-1}, and $C_3 = 0.1$ fm. This form was adopted in a variational Monte Carlo treatment [31] of the ground state of symmetrical nuclear matter based on the v_2 potential, which is given by the central part of the Reid soft-core interaction in the $^3S_1$–$^3D_1$ channel, acting in *all* partial waves [28,29,31]. The stated parameter values correspond to a minimization of the Jastrow-Slater energy expectation value.

The "Gaussian" model (designated G2) is defined by the choice

$$f(r) = 1 - \exp(-\beta^2 r^2) \qquad \text{(G2)} \quad (20)$$

with $\beta = 1.478$ fm^{-1}. This model has no direct connection with any familiar two-nucleon interaction. Evidently, however, it should be associated with a potential containing a soft repulsive core—softer than the Yukawa core present in the v_2 interaction.

Both models were employed in the study of Flynn *et al.* [32], which compared various methods for numerical evaluation of the momentum distribution $n(p)$ for a Jastrow-Slater wave function; these models were also used in the recent low-cluster order calculations [5] of the generalized momentum distribution $n(\mathbf{p}, \mathbf{Q})$.

The two models for the Jastrow two-body correlations are depicted in Fig. 1. The MC and G2 correlation functions show significant differences in behavior both in the inner region and at medium distances. Most notably, the MC function has a considerably larger "correlation hole." A salient measure of the difference between the two models is the wound parameter $\kappa_{\rm dir} = \rho \int [f(r) - 1]^2\, d\mathbf{r}$, whose magnitude quantifies the strength of the correlations in terms of their effectiveness in depleting the Fermi sea [25,28,32]. For the two models we have $\kappa_{\rm dir} = 0.297$ (MC) and 0.111 (G2).

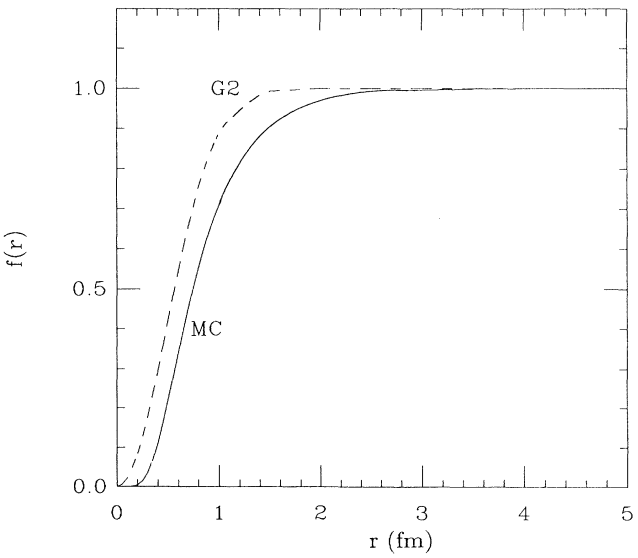

FIG. 1. Pair correlation functions $f(r)$ defining the Monte Carlo (MC) and Gaussian (G2) models of the correlation structure of nuclear matter, plotted against radial distance r [see Eqs. (19) and (20)].

IV. NUMERICAL RESULTS

It is seen from the result (12), or from the sequential relation (9), that at $Q = 0$ the generalized momentum distribution function just reproduces the single-particle momentum distribution $n(p)$, with the large factor $A - 1$. Therefore our numerical investigation is addressed to the nontrivial portion of $n(\mathbf{p}, \mathbf{Q})$ that enters when $Q \neq 0$. This quantity is of order unity compared to A. Its counterpart for the noninteracting system is simply $-\Theta(k_F - p)\Theta(k_F - |\mathbf{p} - \mathbf{Q}|)$, i.e., -1 when p and $|\mathbf{p} - \mathbf{Q}|$ are both within the Fermi sphere, and zero otherwise.

Disregarding $n^{(3)'}$, the FHNC/0 approximation has been employed to construct the dimensionless quantity $n(\mathbf{p}, \mathbf{Q})$ at $Q \neq 0$ from Eq. (12) at selected points in the ranges $[0, 3k_F]$ and $(0, 4k_F]$ of the momentum variables p and Q, respectively. In presenting results, we shall focus on the case in which $\mathbf{p}$ and $\mathbf{Q}$ are parallel. In Ref. [5], the dependence of $n(\mathbf{p}, \mathbf{Q})$ on the angle $\theta_{\mathbf{p},\mathbf{Q}}$ between $\mathbf{p}$ and $\mathbf{Q}$ was studied for the MC model in lowest-cluster-order (LO) approximation. Similar behavior is to be expected in the FHNC/0 treatment. In particular, for $p = k_F$ and $Q < 2k_F$, the LO estimate of $-n(\mathbf{p}, \mathbf{Q})$ is maximal at $\theta_{\mathbf{p},\mathbf{Q}} = 0$.

Figure 2 provides a view of $n(\mathbf{p}, Q\mathbf{p}/p)$ for the MC model as given by the FHNC/0 approximation. The sharp structural features of the corresponding picture in Ref. [5] are now absent and accordingly should be regarded as artifacts of the LO approximation and/or of the interpolation routine used. (We note that in either case the Fermi discontinuities seen in Figs. 3–5 and 7–9 are not well represented in the contour plots.) Some numerical results from the FHNC/0 calculation are reported in Table I. Figures 3 and 4 display $n(\mathbf{p}, Q\mathbf{p}/p)$ as a function of Q at $p = k_F^-$ and $p = 2k_F$, respectively, the results for the MC and G2 models being compared with that for noninteracting fermions. It should be noted that for $p < k_F$ the function $n(\mathbf{p}, Q\mathbf{p}/p)$ is discontinuous at $Q = p + k_F$, and deviations of $-n(\mathbf{p}, Q\mathbf{p}/p)$ from unity for $Q < p + k_F$ and from zero for $Q > p + k_F$ measure the effects of dynamical correlations. Dynamical correlations are also responsible for any nonvanishing values of $n(\mathbf{p}, \mathbf{Q})$ when $p > k_F$. In this p range, $n(\mathbf{p}, Q\mathbf{p}/p)$ has discontinuities at $Q = p - k_F$ and $Q = p + k_F$. As expected from the relative sizes of the wound parameters associated with the two nuclear-matter models, the calculated departures from the Fermi gas limit are generally somewhat larger for the MC model than for G2.

Referring once again to Eq. (12), we denote the term $(1-\delta_{Q0})F_{dd}(Q)n(p)$ and its time-reversed counterpart by t_1 and t_2, respectively; the term $(1 - \delta_{Q0})F_{de}(Q)n_{Dl}(p)$ and its time-reversed partner, by t_3 and t_4, respectively; the term $-n_0(1-\delta_{Q0})[\Theta(k_F - p) - F_{cc}(p)][\Theta(k_F - |\mathbf{p} - \mathbf{Q}|) - F_{cc}(|\mathbf{p} - \mathbf{Q}|)]$, by t_5; and the term $(1 - \delta_{Q0})n^{(2)'}(\mathbf{p}, \mathbf{Q})$, by t_6. Figure 5 furnishes information on the numerical contributions of the addends t_1, t_3, t_5, and t_6 for the case $p = k_F^-$ in the MC model. In this case, t_2 is nearly equal to t_1 for $Q < 2k_F$ but much smaller than t_1 when $Q > 2k_F$, due to the discontinuous behavior of the momentum distribution $n(|\mathbf{p} - \mathbf{Q}|)$. [According to Fig. 6, the function $n(k)$ remains close to 0.85 for $k < k_F$ and is considerably less than unity for $k > k_F$.] The corresponding statement holds for t_4 relative to t_3, since the modified momentum distribution $n_{Dl}(k)$ has the same qualitative behavior as $n(k)$ (again

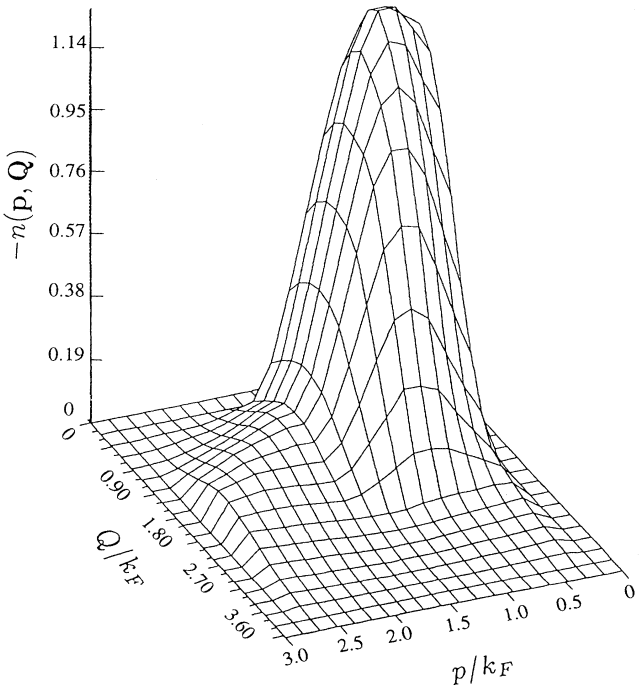

FIG. 2. Generalized momentum distribution $n(\mathbf{p}, \mathbf{Q})$ as a function of momentum variables p and Q (> 0) for $\mathbf{p}$ parallel to $\mathbf{Q}$, calculated by the FHNC/0 procedure based on MC correlations and nucleon density $\rho = 0.182$ fm^{-3}.

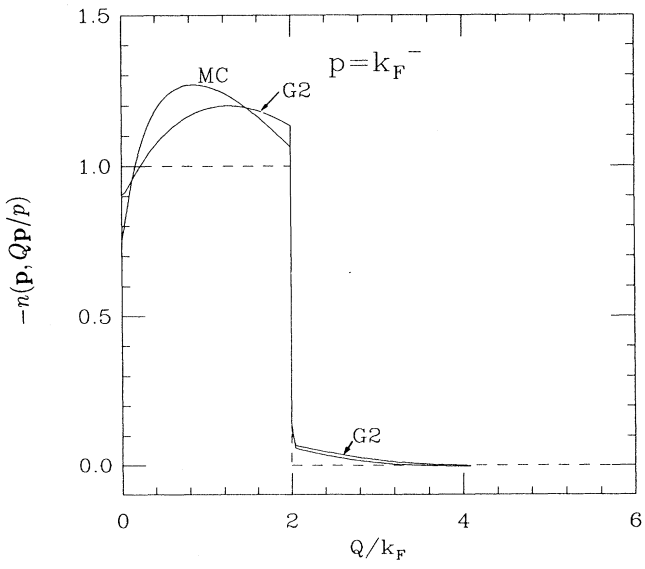

FIG. 3. Generalized momentum distribution $n(\mathbf{p}, \mathbf{Q})$ as a function of Q (> 0) for $\mathbf{Q} \| \mathbf{p}$ and $p = k_F^-$, calculated by the FHNC/0 procedure based on the MC and G2 models and nucleon density $\rho = 0.182$ fm^{-3}. The result for the ideal Fermi gas (dashed curve) is included for comparison.

TABLE I. Values of the generalized momentum distribution $n(\mathbf{p}, Q\mathbf{p}/p)$ of nuclear matter at nucleon density $\rho = 0.182$ fm^{-3} obtained for the MC choice of correlations using the FHNC/0 method.

				p/k_F				
Q/k_F	0	0.5	1.0^-	1.0^+	1.5	2.0	2.5	3.0
0^+	-0.7858	-0.7768	-0.7517	0.0909	-0.0067	-0.0015	-0.0002	0.0001
0.5^-	-1.2396	-1.2326	-1.2226	-0.2337	-0.0233	-0.0085	-0.0028	-0.0008
0.5^+					-0.1628			
1.0^-	-1.2625	-1.2603	-1.2634	-0.1772	-0.1910	-0.0142	-0.0053	-0.0018
1.0^+	-0.1763					-0.1943		
1.5^-	-0.1532	-1.1824	-1.1876	-0.2067	-0.1551	-0.1664	-0.0077	-0.0032
1.5^+		-0.1255					-0.1719	
2.0^-	-0.1048	-0.0876	-1.0633	-0.0611	-0.0901	-0.1078	-0.1178	-0.0134
2.0^+			-0.0610	-0.0088				-0.1227
2.5^-	-0.0591	-0.0477	-0.0293	-0.0009	-0.0304	-0.0502	-0.0630	-0.0702
2.5^+					-0.0066			
3.0^-	-0.0293	-0.0217	-0.0092	0.0019	-0.0016	-0.0113	-0.0251	-0.0337
3.0^+						-0.0032		
3.5^-	-0.0117	-0.0073	0.0006	0.0028	0.0004	-0.0006	-0.0022	-0.0113
3.5^+							-0.0017	
4.0^-	-0.0022	0.00003	0.0043	0.0032	0.0012	0.0003	-0.0003	0.0012
4.0^+								-0.0009

see Fig. 6). Indeed, the terms t_1 and t_3 are of comparable size, though of opposite sign because of the opposite signs of the form factors $F_{dd}(Q)$ and $F_{de}(Q)$. Like t_2 and t_4, the term t_5 exhibits a discontinuity at $Q = p + k_F = 2k_F$, in this instance because of the presence of the step function $\Theta(k_F - |\mathbf{p} - \mathbf{Q}|)$. It is to be recalled that t_5 is not purely dynamical in origin, as it incorporates the second term of the result (4) for noninteracting fermions.

The term t_6 (corresponding to $n^{(2)'}$) is seen to be virtually negligible. In fact, it is found to be much smaller than unity in all kinematic combinations so far considered. Moreover, in those cases where t_6 is not a negligible contributor to $n(\mathbf{p}, \mathbf{Q})$, all the terms are small and prone to numerical error. These findings afford some support for the omission of $n^{(3)'}$ from the calculation. If the density and correlation strength are such that the simpler of the two three-point quantities (nonseparable, but built entirely from two-point quantities) is small, then, by virtue of its density dependence and its involvement of intrinsically three-point functions, the more complicated object $n^{(3)'}$ can be expected to be even less important.

In comparing the detailed composition of FHNC/0, LO, and LOIC1 approximations for $n(\mathbf{p}, \mathbf{Q})$, what is most important is that neither of the "lowest-order" cluster treatments [5] includes any contribution from the exchange-scattering portion of Eq. (12), since $F_{de}(Q)$ contains no two-body part. In other words, the earlier

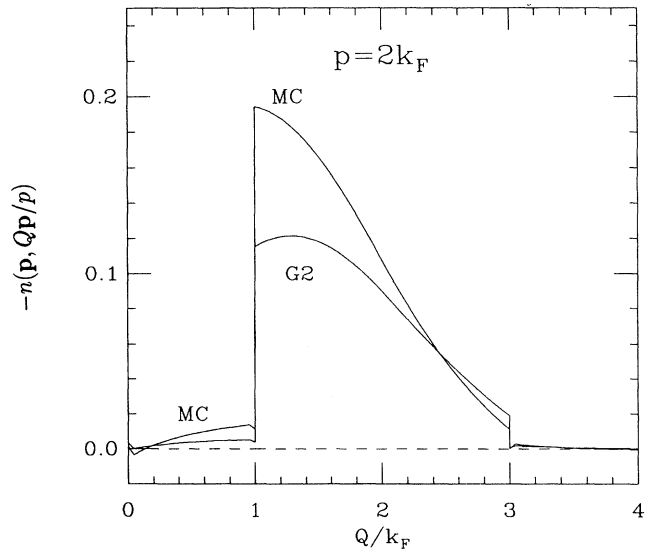

FIG. 4. As in Fig. 3 but at $p = 2k_F$.

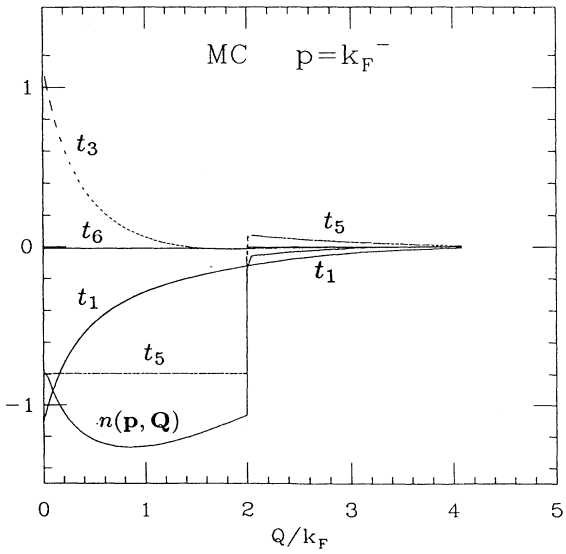

FIG. 5. Contributions t_1, t_3, t_5, and t_6 to $n(\mathbf{p}, \mathbf{Q})$, evaluated in FHNC/0 approximation as functions of Q (> 0) for $\mathbf{Q} \| \mathbf{p}$ and $p = k_F^-$, based on the MC model and density $\rho = 0.182$ fm^{-3}. The full $n(\mathbf{p}, Q\mathbf{p}/p)$ for this case is plotted for comparison.

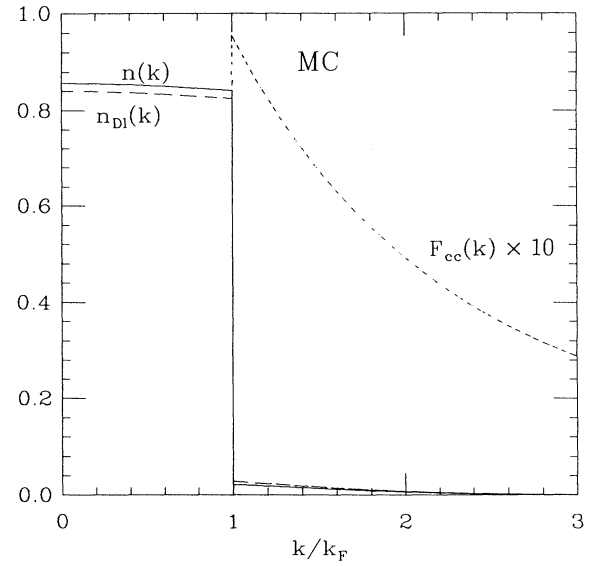

FIG. 6. Momentum distribution $n(k)$, modified momentum distribution $n_{Dl}(k)$, and circular-exchange form factor $F_{cc}(k)$, as functions of k, calculated in FHNC/0 approximation for the MC model and density $\rho = 0.182$ fm^{-3}. The function $F_{cc}(k)$ vanishes for $k < k_F$.

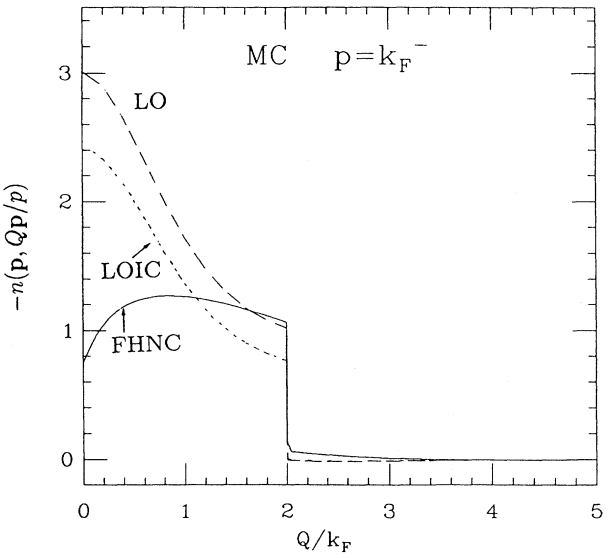

FIG. 7. Comparison of lowest-order cluster (LO), lowest-order irreducible cluster (LOIC1), and Fermi hypernetted-chain (FHNC/0) approximations to the generalized momentum distribution $n(\mathbf{p}, Q\mathbf{p}/p)$, displayed as functions of Q (> 0) at $p = k_F^-$ for the MC model and density $\rho = 0.182$ fm^{-3}. The long- and short-dashed curves are indistinguishable for $Q > 2k_F$.

calculations omit the quantity $t_3 + t_4$, which, as in the example of Fig. 5, can be substantial. Indeed, in that example $t_3 + t_4$ largely compensates $t_1 + t_2$ for $p < 2k_F$ and quenches an otherwise inordinately large departure from the Fermi-gas result. Detailed inspection of the numerical values of the other terms in Eq. (12) shows no dramatic disagreement between FHNC/0 and cluster evaluations, other than in cases where the terms involved are very small. This statement applies to both MC and G2 models across the range of kinematic conditions examined, although a sensitivity to the size of the wound parameter $\kappa_{\rm dir}$ is certainly apparent, higher-order corrections being smaller for G2 than for MC.

The overall numerical discrepancies between the Fermi hypernetted-chain and cluster-truncation results for $n(\mathbf{p}, \mathbf{Q})$ are exemplified in Figs. 7 and 8 for the MC model at $p = k_F^-$ and $2k_F$, respectively. Higher-order contributions present in the FHNC/0 treatment [and due predominantly to the exchange-scattering term of Eq. (12)] evidently have a net large positive effect at low Q (Fig. 7) or low $Q - k_F$ (Fig. 8) which greatly reduces the amplitude of the correlation correction to the Fermi-gas limit.

The quantitative inadequacy of the LO and LOIC1 calculations of Ref. [5] is signaled by large violations of the sequential relation (9). Discrepancies from this basic condition are conveniently measured by a quantity ΔS, obtained by adding $n(p)$ to the left side of Eq. (18), dividing the result by $n(p)$, and expressing the quotient as a percentage. To cite typical examples, the three approximation schemes show the following violations at $p = k_F^-$: $\Delta S = -272.6\%$ (LO), -192% (LOIC1), and $+7.2\%$ (FHNC/0) for the MC model and $\Delta S = -62.9\%$ (LO), -47.3% (LOIC1), and 2.2% (FHNC/0) for the G2 model.

For all cases examined, use of the FHNC/0 algorithm in place of the lowest-order cluster prescriptions leads to dramatic improvement toward satisfaction of the sequential relation. The remaining violations are of modest size and depend on $\kappa_{\rm dir}$ in the expected manner (i.e., larger deviations are associated with the larger $\kappa_{\rm dir}$). These discrepancies may be traced to the neglect of all elementary diagrams and of the $n^{(3)'}$ term of Eq. (12). At this point it is not clear which omission is the more serious.

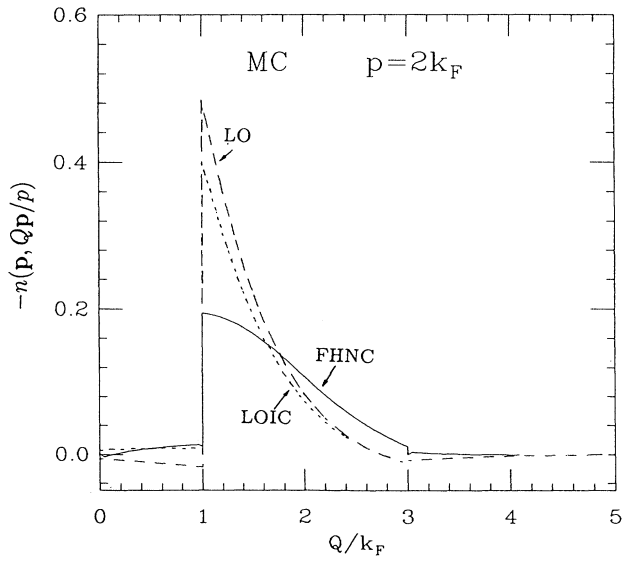

FIG. 8. As in Fig. 7 but at $p = 2k_F$. The long- and short-dashed curves are indistinguishable for $Q > 2.5k_F$.

On the basis of the above findings, we may propose simple extensions of the LO and LOIC1 approximations that will substantially broaden their applicability. The LO approximation should be supplemented by the leading *nonzero* cluster contribution to the exchange-scattering component of Eq. (12) (i.e., to the t_3+t_4 term), implying the addition of certain three-body cluster diagrams. Similarly, the LOIC1 approximation as defined in Ref. [5] should be modified to allow for a nonzero form factor $F_{de}(Q)$ by including its three-body cluster contributions.

It is of interest to compare the FHNC/0 evaluation of the generalized momentum distribution with the simple formula (10) employed by Silver [23] in his hard-core perturbation theory of final-state interactions. For the inputs $n(p)$ and $S(Q)$ to the Ansatz (10) we take the FHNC/0 versions of these quantities calculated for the MC model. In Fig. 9 the comparison is made for $\mathbf{Q}\|\mathbf{p}$ at $p = k_F^-$. The Silver estimate of $-n(\mathbf{p},\mathbf{Q})$ lies considerably below the FHNC/0 result in the "Fermi gas" regime specified by $p \leq k_F$ and $|\mathbf{p}-\mathbf{Q}| \leq k_F$, and it misses the discontinuities implied by the Pauli kinematic effect. Moreover, as already indicated, this approximation breaks time-reversal invariance, which is manifestly preserved in the FHNC/0 treatment. Figure 10 provides further insight into the shortcomings of approximation (10), along with information on the behavior of the sum of form factors $F_{dd}(k)+F_{de}(k)$. In Silver's estimate, the latter sum is replaced by $S(k)-1$, which is clearly a poor assumption for small k.

For a Fermi system modeled by a Jastrow-Slater wave function, the Fermi cancellation phenomenon [28] leads to the conditions [4] $F_{dd}(k=0)+F_{de}(k=0)=0$ and $S(k=0)=0$. The deviations from these exact relations observed in Fig. 10, which may be ascribed to the omission of elementary diagrams in the FHNC/0 calculations, are consistent with the relatively minor violation of the sequential relation quoted above for the MC model.

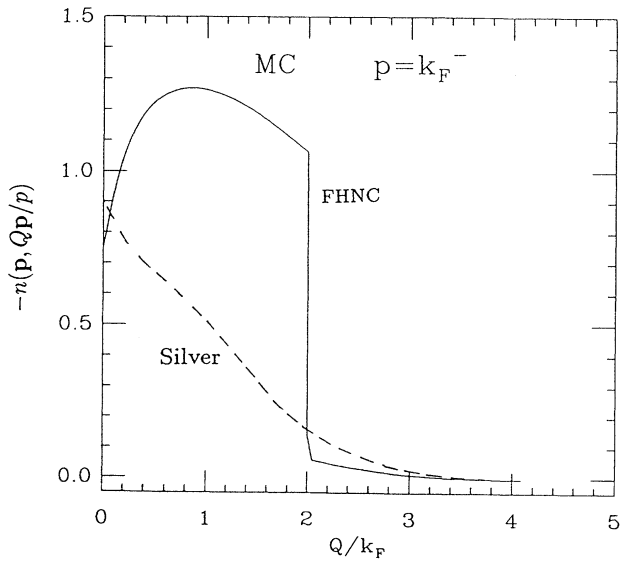

FIG. 9. Generalized momentum distribution $n(\mathbf{p}, Q\mathbf{p}/p)$ as a function of Q (>0) at $p = k_F^-$, as calculated from Silver's formula (10) and in FHNC/0 approximation, for the MC model and $\rho = 0.182$ fm^{-3}.

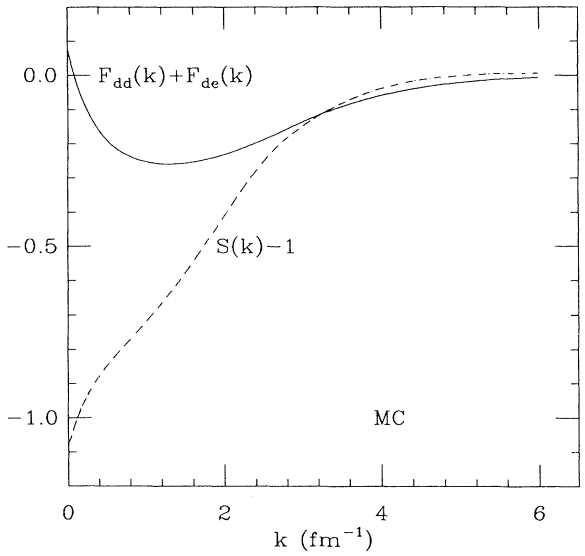

FIG. 10. Comparison of FHNC/0 results for the quantities $F_{dd}(k)+F_{de}(k)$ and $S(k)-1$, computed for the MC model and $\rho = 0.182$ fm^{-3}. Here, $F_{dd}(k)$ and $F_{de}(k)$ are form factors entering the structural expression (12) and $S(k)$ is the static structure function.

Along with the aforementioned replacement, Silver's formula (10) for the generalized momentum distribution entails identification of the full Fermi momentum distribution $n(p)$ with the modified distribution $n_{Dl}(p)$ and replacement of the circular-exchange form factor $F_{cc}(p)$ by the step function $\Theta(k_F-p)$ (see Ref. [4]). The latter simplification amounts to omission of the Pauli-exclusion correction to $n(\mathbf{p},\mathbf{Q})$. The merits and demerits of these two aspects of approximation (10) may be judged from Fig. 6.

Finally, it is useful to consider a coordinate-space view of the information contained in Fig. 10. The Fourier inverses $F_{dd}(r)+F_{de}(r)$ and $g(r)-1$ of the quantities in Fig. 10 are compared in Fig. 11, where we note that the former function has a significantly smaller correlation hole than the latter at short distance, corresponding to a significantly smaller excluded volume. The same feature is seen in liquid ^{3}He [4].

This observation is relevant to a recent study of final-state interactions in inclusive (e,e') scattering from nuclear matter carried out within correlated Glauber theory [11]. In the treatment of Benhar *et al.* [11], further expounded in Refs. [12,13], the recoiling nucleon is described relativistically, and its final-state interactions are calculated by means of a generalized Glauber multiple-scattering theory in which the nucleon propagates through the same *correlated* medium to which it was bound before being hit by the electron. Accordingly, the struck nucleon in the initial state is surrounded by a correlation hole. This correlation hole, corresponding to a region of reduced nucleonic density, has the consequence

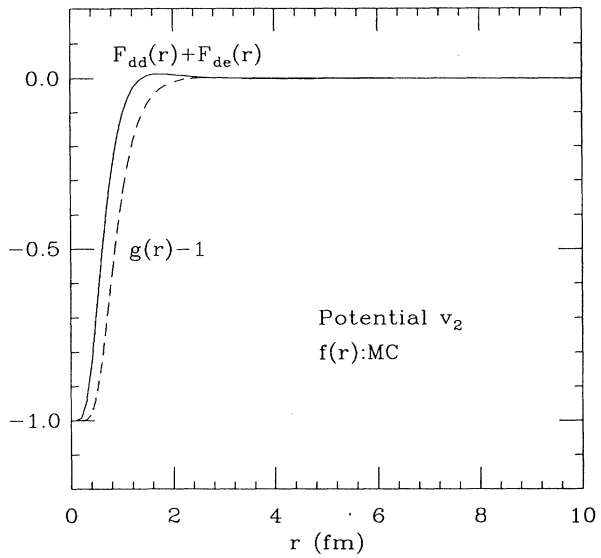

FIG. 11. The comparison of Fig. 10 is repeated in coordinate space, $g(r)$ being the radial distribution function corresponding to the static structure function $S(k)$.

that the recoiling nucleon experiences little damping at short distances ($\lesssim 1$ fm) from the interaction site. Hence the short-range correlations produce an effect qualitatively similar to that of color transparency [33–35]. It follows that if convincing conclusions are to be drawn from experiment regarding the quantitative importance of color transparency in inclusive scattering of GeV electrons, it will be necessary to make an accurate accounting of this analogous effect of short-range nucleon-nucleon correlations, with the half-diagonal two-body density matrix as the natural descriptor.

The approach of Benhar *et al.* approximates the effects of ground-state correlations on the inclusive scattering in essentially the same manner as Silver, who replaces $F_{dd}(r)+F_{de}(r)$ by $g(r)-1$. The calculations performed in Ref. [11] reveal a pronounced sensitivity of the inclusive cross section to the size of the hole in the input radial distribution function $g(r)$, particularly at small energy loss ω. The comparison drawn in Fig. 11 should provide further impetus to a more thorough investigation of the role of the half-diagonal two-body density matrix in the determination of final-state corrections and a more realistic evaluation of this important quantity.

V. CONCLUSIONS

In summary, we have applied Fermi-hypernetted chain theory to achieve quantitative microscopic determination of a momentum-space transform $n(\mathbf{p},\mathbf{Q})$ of the half-diagonal two-body density matrix of nuclear matter, in the restricted context of a ground-state trial function containing only state-independent, central, two-body correlations. The results exhibit interesting features that reflect the interplay of statistical and geometrical correlations. Further investigations of $\rho_{2h}(\mathbf{r}_1,\mathbf{r}_2,\mathbf{r}_1')$ and $n(\mathbf{p},\mathbf{Q})$ in nuclear matter should extend the analysis and the calculations to the case of realistic, state-dependent correlations. Some progress in this direction has been made recently by Gearhart [36] within self-consistent Green's function theory. A second important direction for future work is the microscopic determination of these functions in finite nuclear systems. In analogy with an earlier study [37] of the momentum distribution $n(p)$ in finite nuclei, it may be fruitful to apply a suitable local-density approximation based on inputs from the evaluation of $\rho_{2h}(\mathbf{r}_1,\mathbf{r}_2,\mathbf{r}_1')$ in (uniform) nuclear matter over a range of densities. To this end, an extension of the local-density approximation proposed by Có, Fabrocini, and Fantoni [38] for the one-body density matrix might be developed.

ACKNOWLEDGMENTS

We have benefited from discussions with W. H. Dickhoff, S. Fantoni, G. Orlandini, A. S. Rinat, M. L. Ristig, and M. Traini. The research reported in this paper has been supported in part by the Greek Secretariat of Research and Development under Contract No. 360/91 and by the U.S. National Science Foundation under Grant No. PHY-9307484. M.P. thanks the Bodossaki Foundation for financial support.

[1] A. N. Antonov, P. E. Hodgson, and I. Zh. Petkov, *Nucleon Momentum and Density Distributions in Nuclei* (Clarendon Press, Oxford, 1988).

[2] *Momentum Distributions*, edited by R. N. Silver and P. E. Sokol (Plenum Press, New York, 1989).

[3] C. Ciofi degli Atti, E. Pace, and G. Salmè, Phys. Rev. C **43**, 1155 (1991).

[4] M. L. Ristig and J. W. Clark, Phys. Rev. B **41**, 8811 (1990).

[5] J. W. Clark, E. Mavrommatis, and M. Petraki, Acta Phys. Pol. **24**, 659 (1993) [Janusz Dąbrowski Festschrift Issue].

[6] B. Frois and C. Papanicolas, Annu. Rev. Nucl. Part. Sci. **37**, 133 (1987); D. B. Day, J. S. McCarthy, T. W. Donnelly, and I. Sick, *ibid.* **40**, 357 (1990); L. L. Frankfurt, M. I. Strikman, D. B. Day, and M. Sargsyan, Phys. Rev. C **48**, 2451 (1993).

[7] P. K. A. de Witt Huberts, J. Phys. G **16**, 507 (1990); L. Lapikás, Nucl. Phys. **A553**, 297c (1993).

[8] L. Kester, *Investigation of Short Range Correlations in ^{12}C with the $(e,e'p)$ and $(e,e'pp)$ Reactions* (Elinkwijk b.v., Utrecht, 1993) [Ph.D. thesis, Vrije Universiteit, Amsterdam, 1993].

[9] A. S. Carroll, D. S Barton, G. Bunce, S. Gushue, Y. I. Makdisi, S. Heppelmann, H. Courant, G. Fang, K. J. Heller, M. L. Marshak, M. A. Shupe, and J. J. Russel, Phys. Rev. Lett. **61**, 1698 (1988).

[10] D. Ashery and J. P. Schiffer, Annu. Rev. Nucl. Part. Sci.

36, 207 (1986).
[11] O. Benhar, A. Fabrocini, S. Fantoni, G. A. Miller, V. R. Pandharipande, and I. Sick, Phys. Rev. C **44**, 2328 (1991).
[12] O. Benhar, A. Fabrocini, S. Fantoni, V. R. Pandharipande, and I. Sick, Phys. Rev. Lett. **69**, 881 (1992).
[13] S. Fantoni and I. Sick, in *Electron-Nucleus Scattering*, EIPC, Italy, edited by O. Benhar, A. Fabrocini, and R. Schiavilla (World Scientific, Singapore, 1994), p. 88.
[14] V. R. Pandharipande and S. C. Pieper, Phys. Rev. C **45**, 791 (1992).
[15] O. Benhar and V. R. Pandharipande, Phys. Rev. C **47**, 2218 (1993).
[16] A. Kohama, K. Yazaki, and R. Seki, Nucl. Phys. **A551**, 687 (1993).
[17] N. N. Nikolaev, A. Szczurek, J. Speth, J. Wambach, B. G. Zakharov, and V. R. Zoller, Phys. Lett. B **317**, 281 (1993).
[18] J. W. Clark and R. N. Silver, in *Proceedings of the Fifth International Conference on Nuclear Reaction Mechanisms*, edited by E. Gadioli (Universitá degli Studi di Milano, Milan, 1988), p. 531.
[19] A. S. Rinat and W. H. Dickhoff, Phys. Rev. B **42**, 10 004 (1990).
[20] S. Stringari, Phys. Rev. B **46**, 2974 (1992).
[21] M. L. Ristig and J. W. Clark, Phys. Rev. B **40**, 4355 (1989).
[22] H. A. Gersch, L. J. Rodriguez, and P. N. Smith, Phys. Rev. A **5**, 1547 (1972).
[23] R. N. Silver, Phys. Rev. B **38**, 2283 (1988).
[24] A. S. Rinat, Phys. Rev. B **40**, 6625 (1989).
[25] M. L. Ristig and J. W. Clark, Phys. Rev. B **14**, 2875 (1976).
[26] S. Fantoni, Nuovo Cimento A **44**, 191 (1978).
[27] M. L. Ristig, in *From Nuclei to Particles*, Proceedings of the International School of Physics "Enrico Fermi," Course LXXIX, Varenna, 1980, edited by A. Molinari (North-Holland, Amsterdam, 1982), p. 340.
[28] J. W. Clark, in *Progress in Particle and Nuclear Physics*, Vol. 2, edited by D. H. Wilkinson (Pergamon Press, Oxford, 1979), p. 89.
[29] V. R. Pandharipande and R. B. Wiringa, Rev. Mod. Phys. **51**, 821 (1979).
[30] J. W. Clark and E. Krotscheck, Lecture Notes in Phys. **198**, 127 (1984).
[31] D. Ceperley, G. V. Chester, and M. H. Kalos, Phys. Rev. B **16**, 3081 (1977).
[32] M. F. Flynn, J. W. Clark, R. M. Panoff, O. Bohigas, and S. Stringari, Nucl. Phys. **A427**, 253 (1984).
[33] S. J. Brodsky, in *Proceedings of the Thirteenth International Symposium on Multiparticle Dynamics*, Volendam, The Netherlands, 1982, edited by E. W. Kittel, W. Metzger, and A. Stergion (World Scientific, Singapore, 1982), p. 963.
[34] A. Mueller, in *Proceedings of the Seventeenth Rencontre de Moriond*, Les Arcs, France, 1982, edited by J. Tran Thanh Van (Editions Frontières, Gif-sur-Yvette, 1982), p. 13.
[35] L. L. Frankfurt and M. I. Strikman, Phys. Rep. **160**, 235 (1988).
[36] C. C. Gearhart, Ph.D. thesis, Washington University, St. Louis, 1994.
[37] S. Stringari, M. Traini, and O. Bohigas, Nucl. Phys. **A516**, 33 (1990).
[38] G. Có, A. Fabrocini, and S. Fantoni, Nucl. Phys. **A568**, 73 (1994).